Nature Environment and Pollution Technology
An International Quarterly Scientific Journal

p-ISSN: 0972-6268
(Print copies up to 2016)
e-ISSN: 2395-3454

Vol. 21 | No. 1 | pp. 339-347 | 2022

Original Research Paper

https://doi.org/10.46488/NEPT.2022.v21i01.041

Open Access Journal

Low-Cost Calibration MOS Gas Sensor for Measuring SO_2 Pollutants in Ambient Air

R. Purbakawaca*†, A.S. Yuwono, I.D.M. Subrata* and H. Alatas*****

*Department of Mechanical and Biosystems Engineering, IPB University, Bogor, 16680, Indonesia
**Department of Civil and Environmental Engineering, IPB University, Bogor, 16680, Indonesia
***Department of Physics, IPB University, Bogor, 16680, Indonesia
†Corresponding author: R. Purbakawaca; purbakawaca09rady@apps.ipb.ac.id

Nat. Env. & Poll. Tech.
Website: www.neptjournal.com

Received: 09-05-2021
Revised: 30-06-2021
Accepted: 15-07-2021

Key Words:
SO_2 gas sensor
Gas sensor calibration
Low-cost gas calibration
Voltage response MOS
Raw signal MOS

ABSTRACT

Air pollution has evolved into a global issue that necessitates immediate and accurate pollution control. The usage of the Metal Oxide Semiconductor (MOS) sensor as a monitoring system for air pollution levels is one possible answer to this challenge. The MQ-136 sensor is calibrated using standard SO_2 (0, 5, 10, 20, 30, 40, 50, 60, 70) ppm as the test gas in this study. To collect the sensor output signal, a variety of equipment was created, including a gas test box, a voltage divider, and follower circuit, and a gas flow control unit operated by a microcontroller. The test gas can be pumped into the test box at a constant rate of 1.0 $L.min^{-1}$ by the apparatus. To evaluate a significant difference (= 0.05), an analysis of variance was performed on the response signal generated by a series of sensors due to the concentration of the test gas. To examine the correlation between the sensor response signal and the test gas concentration treatment, as well as the sensor performance, linear regression analysis was used. The ANOVA results demonstrate no significant differences amongst the sensors, indicating that they all follow the same routine. Furthermore, ANOVA analysis reveals that the sensors respond differently at each level of SO_2 concentration. According to linear regression, the relationship between gas concentration and sensor-1, sensor-2, and sensor-3 output signals is reflected by coefficients of determination of 0.94, 0.91, and 0.93, respectively.

INTRODUCTION

Air pollution has become a global problem given the risk it poses to human health and the environment. Air pollution is increasing as a result of rapid urbanization, industrialization, population, and economic growth (Rumana et al. 2014). Air pollution has been found to have harmful consequences on human health and the environment in recent studies. Air pollution, for example, has a social and economic impact on crop yields in developing countries (Ahmed 2015).

Measurement of SO_2 is an important component of air pollution control initiatives. Fossil fuels, refining and combustion, non-ferrous smelting, iron ore smelting, pulp, and paper mills, transportation sources, and steel mills all contribute about 99 per cent of sulfur dioxide to the environment (Riordan & Adeeb 2004). These pollutants, when emitted in high quantities into the ambient air, can cause health problems such as pulmonary, asthma, and other respiratory illnesses.

Many countries have set guidelines for determining the level of pollution and its consequences, recognizing the hazards of air pollution. Government legislation and national norms influence air pollution levels in Indonesia. The threshold values for air pollutant levels, as well as the methods and equipment for measuring the level of pollutants in the air, are all defined by these laws. The traditional approach is used because it is accurate and selective to the observed parameters, but it has significant maintenance costs and takes a long time to analyze.

Designing a low-cost air pollutant meter that takes advantage of the potential of a solid-state gas sensor is one viable approach to complement existing methods. Solid-state gas sensors, particularly those based on MOS, have become the industry standard in various household, commercial, and industrial gas sensor systems in recent decades (Liu et al. 2012). The MOS gas sensor is connected to an instrumentation system and a network to monitor pollution levels in real-time (Arroyo et al. 2019). Although MOS gas sensors have been used to assess pollutant levels in the ambient air, the gas detection technique is complicated.

MOS gas sensors have benefits over other types of sensors, according to Korotcenkov (2007), especially in terms of sensitivity, stability, price, and reaction time. However, to assure accuracy, evaluation, and validation of gas sensor

performance, MOS gas sensors must be calibrated (Adithyan et al. 2016). When using MOS sensors as a low-cost air quality monitoring system, several factors must be considered, including producing, transferring, and combining data from numerous sensors, as well as reviewing accuracy and predictions (Snyder et al. 2013). The calibration of gas sensors, on the other hand, is neither cheap nor simple.

The calibration of the MQ-136 sensor with standard gas using the apparatus used in this investigation is presented in this publication. In addition, to learn more about sensor performance, ANOVA and linear analysis were used in this study.

MATERIAL AND METHODS

Experimental Setup

To get the sensor output, a series of equipment was created in this study, including a gas test box, voltage divider, follower circuit, and gas flow control unit operated by a microcontroller, as shown in Fig. 1. As shown in Fig. 2, all these components are combined to form an experimental setup for gas sensor calibration.

The test box is a container for holding the test gas and contains a series of gas sensors installed with a fully functional gas flow system. The test box is made of acrylic material with a bending technique to minimize gas leakage. The test box is in the form of a cube with a volume of free space of 1000 cm^3, as shown in Fig. 3. The test box consists of two parts: the top in the form of a lid and the bottom as a gas storage container. The lid is equipped with a rubber seal, a mount for attaching the gas sensor circuit board, and a seven-pin female connector. The gas container is equipped with a 12VDC fan which functions to homogenize the standard gas in the container, and a pneumatic fitting is installed for the gas line.

The MOS gas sensor used is a low-cost sensor manufactured by Hanwei Electronics Co., Ltd, the MQ-136 variant of three sensors. The MQ-136 sensor was chosen because it has a high sensitivity to H_2S gas and can detect other gases containing sulfur (Zhengzhou 2015). However, more detailed and complete information about these sensors is minimal, especially regarding sensor calibration for SO_2 gas. As a result, the sensor will be tested with SO_2 gas in this study to see how accurate the response signal is to the gas concentration level.

As seen in Fig. 4, the standard circuit on the MQ series sensor consists of two parts, namely the heating circuit (R_H) and the signal output circuit (R_s). When the sensor is activated, the heating component will light up and cause the sensing material to activate so that the electrons on the sensing component's surface move freely. Electrons will react with oxygen in the air around the material, thereby increasing the sensing material's resistance R_s (Barsan et al. 2012). However, when the target gas appears, the oxygen molecules will react with the target gas, which causes the R_S to decrease with the target gas content in the air. When R_S

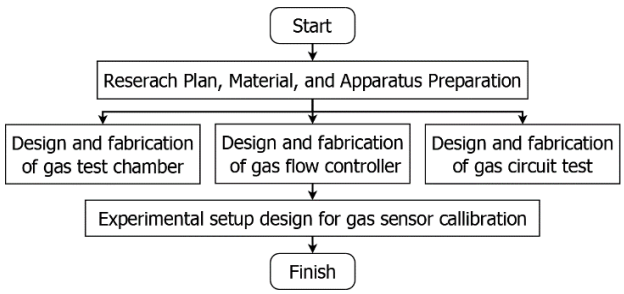

Fig. 1: Design of gas sensor calibration equipment

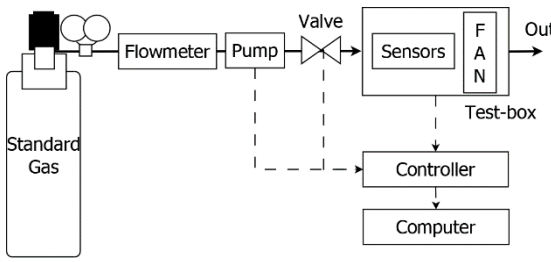

Fig. 2: Experimental setup for low-cost gas sensor calibration.

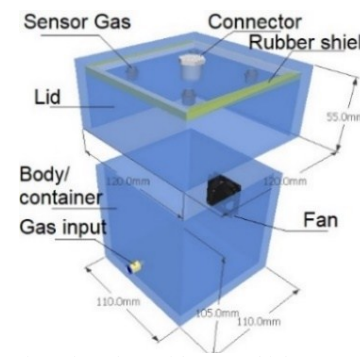

Fig. 3: Design of test box with 5 mm thickness acrylic material.

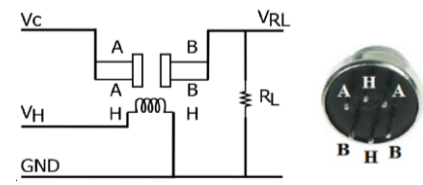

Fig. 4: Illustration of primary test circuit MQ sensor (Zhengzhou 2015).

is combined serially with constant resistance R_L, an electric current is applied due to the potential difference V_C, and there will be a voltage variation V_{RL} due to changes in target gas levels in the air. The relationship between R_S and R_L is described in equation 1.

$$R_S = R_L \left(\frac{V_C}{V_{R_L}} - 1\right) \quad \ldots(1)$$

where V_{RL} is the sensing output (V_0) from the sensor in volt.

The primary test circuit for the MQ sensor above becomes a reference in making the sensor PCB. The suitability of the sensor leads and symbol in Fig. 4 and Fig. 5 is as follows:

a. Pin A is lead numbers 1 and 3, pin B is lead numbers 4 and 6, and pin H is lead numbers 2 and 5.

b. R_L is equivalent to the combination of resistance of R_2 and R_3 or R_5 and R_6 or R_8 and R_9.

c. V_C and V_H represented by V_{CC}.

The gas sensor array system is designed to detect the test gas in the test box. The PCB is designed to mount three sensors at once. R_2, R_5, and R_8 are variable resistors value of 100 kOhm. R_3, R_6, and R_9 have the same resistance value of 1 kOhm. R_1, R_4, and R_5 are used to build a voltage divider with R_H. The MQ sensor manual states that the R_L can be determined as 10 kOhm ± 5%. As shown in Fig. 5, the resistances R_2, R_5, and R_8 are 9 kOhm. So, equation 1 can be rewritten into equation 2.

$$R_S = R_L \frac{(V_{CC} - V_O)}{V_O} \quad \ldots(2)$$

where R_L is the load resistor equivalent $R_2 + R_3$ in kOhm. V_{CC} is applied at 5V.

According to Tian et al. (2005), the MOS sensor output signal, as illustrated in Fig. 6, possesses characteristics with a significant enough gain. Therefore, V_O is observed only by connecting the sensor to the Atmega 328 via a voltage follower circuit as a buffer between the sensor output and the A / D channel. V_O is converted into a digital signal via a 10-bit resolution ADC channel.

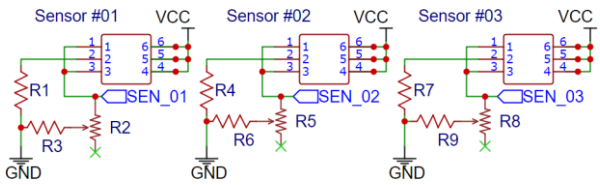

Fig. 5: PCB design for the primary test circuit of the MQ sensor.

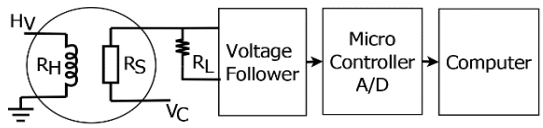

Fig. 6: Interface circuit diagram of MOS gas sensor (Tian et al. 2005).

In this paper, a Moving Average Filter (MAF) is selected as a general denoising method equivalent to low pass filtering (Bassey et al. 2014). MAF works by averaging several points within a specified data point range from the input signal to produce each output signal point described by equation 3.

$$y[k] = \frac{1}{N}\sum_{n=0}^{N-1} x[k+n] \quad \ldots(3)$$

where y is the output signal, N is the number of points of data before the output signal.

This research can obtain the variation in the target concentration level by flowing the standard gas into the test box for a particular duration. This gas flow must be kept constant at 1.0 $L.min^{-1}$ to reach the desired gas concentration. Therefore, the gas standard in the tube is not directly flowed into the test box but through a flow controller in the form of a 12 VDC 5 $L.min^{-1}$ vacuum pump, a Wiebrock 3 KPa 1.5 $NL.min^{-1}$ flowmeter, and a 12 VDC solenoid valve is shown in Fig. 7. The gas flow duration setting is based on a logical button combination. In Table 1, the gas flow duration in code letters will be mapped based on the desired gas concentration in the test box.

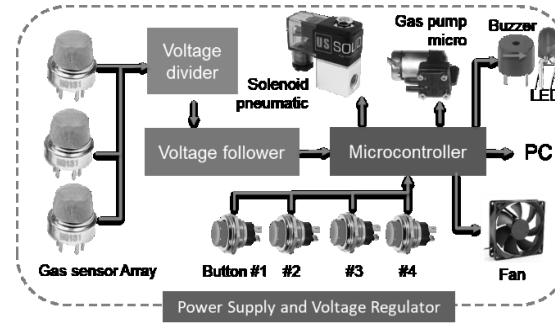

Fig. 7: Electrical schematic of low-cost gas sensor calibration.

Table 1: Logical combination of the button to select a flow duration.

Button				Combination	
B#1	B#2	B#3	B#4	Decimal	Duration
0	0	0	0	0	A
0	0	0	1	1	B
0	0	1	0	2	C
0	0	1	1	3	D
0	1	0	0	4	E
0	1	0	1	5	F
0	1	1	0	6	G
0	1	1	1	7	H
1	0	0	0	8	I

The flow control performance test is conducted to determine the stability of the gas flow. The test was carried out by opening and closing the gas flow rate for 10 repetitions using a flow controller with 100 seconds to flow the gas and 20 seconds to monitor the gas flow. Stability is indicated by the difference in the actual gas flow value on the flowmeter against the target value represented in the Mean Absolute Percentage Error (MAPE) as in equation 4. The same test is also carried out without a flow controller for comparison.

$$MAPE = \frac{1}{N}\sum_{i=1}^{N}\left|\frac{A_i - F_i}{A_i}\right| \quad \ldots(4)$$

where A_i and F_i are the actual and forecast value at data point-i. N is the number of data (Kim & Kim 2016).

Gas Concentration Level

To determine the relationship of the sensor response signal to the treatment of the test gas concentration, Air Liquide standard SO_2 gas is used with a concentration of 100 ppm with an accuracy of 99.0%. The gas concentration in the test box is calculated based on the dilution of the gas as in equation 5. In this study, the range of initial SO_2 gas concentrations is shown in Table 2.

$$C_1 \times V_1 = C_2 \times V_2 \quad \ldots(5)$$

where C_1 is the initial concentration of SO_2 gas, V_1 is the initial volume of SO_2 gas, C_2 is the final concentration SO_2 gas, and V_2 is the final volume SO_2 gas in the test box.

Data Acquisition

Before collecting calibration data, the MQ-136 goes through a preheating phase. The purpose of this step is to determine the nature of the sensor output signal in the target gas condition of 0 ppm in normal settings, as well as the sensor output range and sensor performance similarity. Furthermore, before the initial stage of calibration, the sensor will be turned on for 1 minute at 1-second intervals to establish the sensor's baseline by exposing it to clean air. The data is then subjected to baseline differential modification, as described in equation 7.

$$X_j(t) = V_j(t) - Av_j \quad \ldots(7)$$

where $X_i(t)$ is the corrected raw data value of the sensor-j at time-t, $V_j(t)$ is raw data value of the sensor sensor-j at time-t, and Av_j is mean baseline value of 1 minute.

All stages of the calibration are shown in Fig. 8. First, the test box is cleaned of residue or other contaminant gases by turning on the fan for 5 min, then the lid is closed and stabilizes for 3 min. Next, select the combination to select the gas flow duration and start recording sensor response before gas flows into the test case for 60 seconds. Gas starts flowing by first activating the flow controller. Simultaneously, the fan is turned on for 60 seconds to distribute the gas in the test box evenly. Recording continues for 240 seconds to determine the sensor response after gas flow. Finally, the lid is opened, and the reading is continued for 240 seconds. Repeat all of the above steps three times for the same concentration level and another concentration level. Experiments were carried out in the laboratory by maintaining a temperature of 25 ± 1 °C and relative humidity of 50 ± 5 %.

Table 2: Dilution of SO_2 gas level in normal condition (25°C).

No	Standard SO_2 (ppm)	Flow rate (NL. min^{-1})	Duration time (ms)	Volume target of SO_2 (mL)	Level of SO_2 (ppm)
1	100	1.0	0	0	0
2	100	1.0	3000	50	5
3	100	1.0	6000	100	10
4	100	1.0	12000	200	20
5	100	1.0	18000	300	30
6	100	1.0	24000	400	40
7	100	1.0	30000	500	50
8	100	1.0	36000	600	60
9	100	1.0	42000	700	70

Analysis of Variance and Linear Regression

Analysis of Variance (ANOVA) is a statistical method

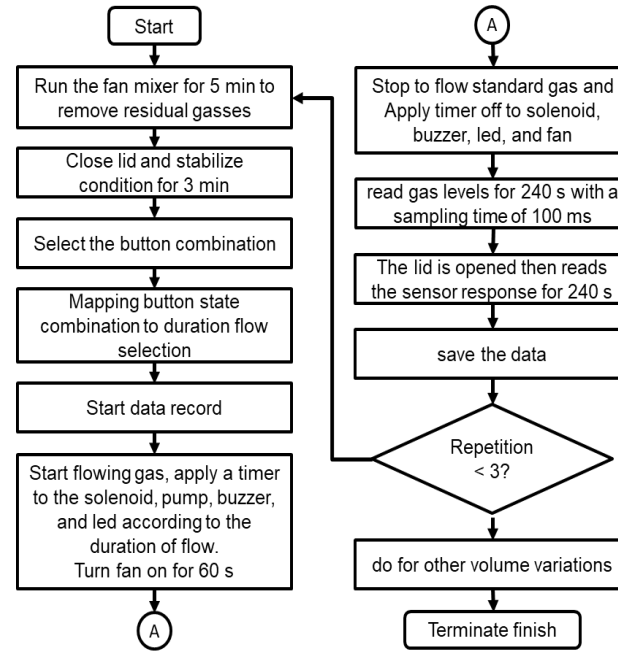

Fig. 8: Workflow of gas sensor calibration.

Table 3: Comparison of the performance stability of flow controller and direct flowing gas.

No	Actual gas flow (f_a) ($L.min^{-1}$)		Target gas flow (f_t) ($L.min^{-1}$)	Error value (%)	
	Flow controller	Direct flowing		Flow controller	Direct flowing
1	1.0	1.0	1.0	0.0	0.0
2	1.1	1.0	1.0	10.0	0.0
3	1.0	1.0	1.0	0.0	0.0
4	1.0	0.9	1.0	0.0	10.0
5	1.0	0.9	1.0	0.0	10.0
6	1.0	0.9	1.0	0.0	10.0
7	1.1	0.8	1.0	10.0	20.0
8	1.0	0.8	1.0	0.0	20.0
9	1.1	0.6	1.0	10.0	40.0
10	1.0	0.6	1.0	0.0	40.0
MAPE				3.0	15.0

commonly used in experimental research. The experimental design was applied using Microsoft Excel software by considering two factors, namely the exposure of the test gas to the sensor gas and the sensor sensitivity, which was calculated from the sensor's response to variations in the concentration of the test gas. ANOVA analysis is used to analyze whether there are differences in the performance of the three sensors from the same sensor variant tested simultaneously and in iteration.

Analysis of Linear Regression

In general, regression analysis is used to determine the relationship between two or more variables (Rawlings et al. 1998). In this study, the gas sensor output signal was chosen as the dependent variable and the variation of the test gas concentration as a predictor variable. The value of the dependent variable can be estimated using the mathematical model defined in equation 8.

$$Y_i = \beta_0 + \beta_1 X_i + \varepsilon_i \quad \ldots(8)$$

Where Y_i shows the concentration of the test gas, X_i is the sensor output signal. β_0 and β_1 are constants. ε_i is a random variable that includes all other factors.

RESULT AND DISCUSSION

Equipment Calibration Performance

The results of standard gas flow rate testing using and without a gas flow controller are shown in Table 3. Comparing the actual data (f_a) with the target gas flow (f_t) using and without a flow controller can determine the MAPE value. The MAPE value system is equipped with a 3.0 % flow controller. Meanwhile, the system direct flowing gas was 15.0 %. Comparing the MAPE values shows that the test gas flow rate using the flow control design is more stable than directly passing the gas into the test box.

Preheating of Gas Sensor

The sensor first goes through a preheating process to achieve chemical equilibrium. The MQ-136 sensor used in this study is still in a new condition, but it is unknown how long it has been in storage since production. Therefore, preheating is essential to avoid instability in the reading of the sensor output signal. In this study, the preheating process was carried out at a test gas concentration level of 0 ppm for 30 hours with an interval of 3 seconds and using a 30 point MAF. MAF with 30 points was chosen because it considers the filter's ability to reduce noise and limited memory Atmega 328.

Fig. 9 shows that the sensor response signal fluctuates and then stabilizes after 24 hours. According to the MQ-136 sensor datasheet, this may be due to the long sensor storage

Table 4: Comparison of the maximum, minimum, average, standard deviation and range values of the three MQ-136 sensors.

Parameter	Sensor-1	Sensor-2	Sensor-3
Mean	876.42	880.06	888.86
Standard Deviation	17.78	29.22	29.88
Range	78.15	139.03	139.03
Minimum	826.05	825.15	834.93
Maximum	904.20	964.18	973.96

time, and the sensor needs time to reach chemical equilibrium through the preheating process. In addition, the fluctuating sensor response can also be caused by changes in temperature and humidity during the preheating process, which affects the basic resistance, sensitivity, and reactivity (Samad et al. 2020). The statistical analysis of the three sensors resulting from the preheating process is presented in Table 4. This shows the similarity of the response signal behavior of the three MQ-136 sensors. In addition, the standard deviation indicates that the data is different from the mean value of each sensor.

Raw Signal Output

The testing of the three MQ-136 sensors was carried out simultaneously at each test gas concentration level of 0, 5, 10, 20, 30,40, 50, 60, and 70 ppm. Sensor testing at each concentration level was repeated three times. Raw data from the sensor output signal for each iteration is digitally processed with the 5-point MAF algorithm on the microcontroller.

Overall, the time taken to test the sensor was 600 seconds. After the sensor is put into the test box, in the time range 0-60 seconds ($t_{0\text{-}60}$), the output signal reads in the condition that SO2 gas has not flowed into the test box, as shown in Fig. 10. This signal shows the baseline condition of the sensor in the range of 0-60 seconds (baseline $t_{0\text{-}60}$) before the test gas is applied. Fig. 11 indicates that the baseline $t_{0\text{-}60}$ values for the three sensors are pretty flat and tend to be the same in each iteration.

The results of the calculation of the mean $t_{0\text{-}60}$ for each sensor are presented in Fig. 12. With a rise in the measured SO_2 concentration, the baseline value of the average $t_{0\text{-}60}$ increases. The sensor response that does not completely recover after recording a given concentration level can cause this increase in the baseline $t_{0\text{-}60}$. In other words, there is still residual test gas on the sensor surface, resulting in a high sensor response value when detecting different concentration levels. In addition, because the gap between repetitions was only 5 minutes, the baseline reading result of $t_{0\text{-}60}$ was higher than before, as shown in Fig. 11.

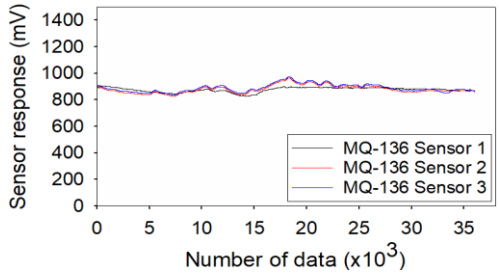

Fig. 9: The baseline value of the MQ-136 sensor is under normal conditions.

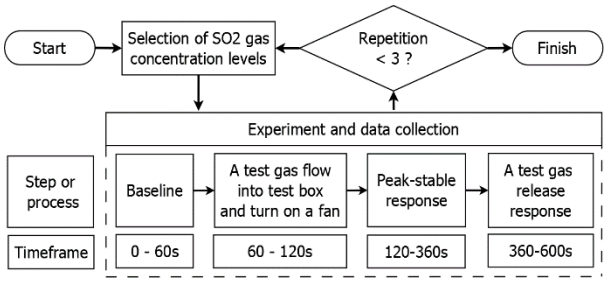

Fig. 10: The baseline value of the MQ-136 sensor is under normal conditions.

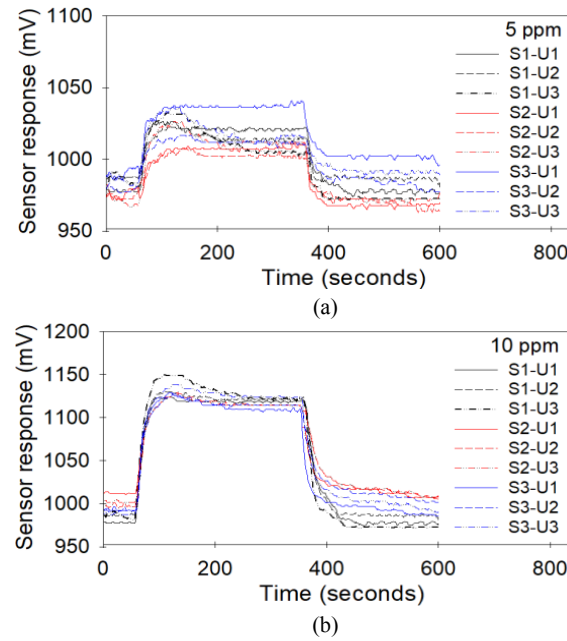

Fig. 11: Raw signal response of sensor MQ-136 for each repetition of each level concentration SO_2 gas in normal condition.

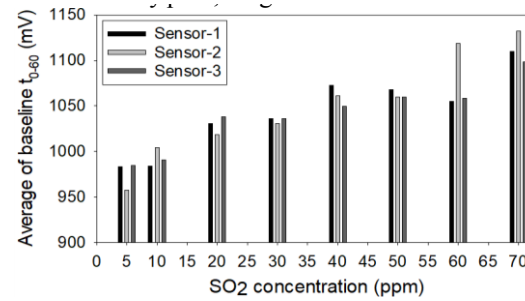

Fig. 12: The average baseline $t_{0\text{-}60}$ value of the MQ-136 for each repetition of each level concentration SO_2 gas.

SO_2 gas is pumped into the test box for 60 seconds, depending on the desired concentration level. The fan is then switched on for 60 seconds to ensure that the gas is evenly spread throughout the box. The response signal rises at the same time until it reaches a steady peak value. The considerable concentration of the test gas influences the sensor's ability to reach a consistent peak time. The longer the output signal from the MQ-136 sensor reaches a steady peak, the greater the concentration value, as illustrated in Fig. 13.

Sensor Response Correction

By using the differential approach, the raw output signal for each sensor is averaged and then corrected by the mean baseline value. As a result, equation 7 corrects the sensor response signal to give it a new range, as shown in Fig. 14, in which each average baseline value subtracts all raw signals from each repetition at each concentration. This is done to account for any variations or changes in sensor response readings and to make comparing sensor output values at different test gas concentration levels easier.

Analysis of Variance

Table 5 shows the mean peak stable signal values at 200-350 second intervals ($t_{200\text{-}350}$) of the corrected data. The time range $t_{200\text{-}350}$ was chosen because almost all of the sensor output signals are stable or flat in that period. The results of data analysis using ANOVA with a significant difference ($\alpha = 0.05$) using Microsoft Excel are presented in Table 7.

Based on Table 6, the term "sample" refers to the MQ-136 sensor group, while the "column" refers to the SO_2 concentration treatment. The sample obtained p-value > 0.05 and $F < F_{crit}$, so it can be said that there is no significant difference in the response signal generated between sensors. In contrast, the column obtained p-value < 0.05 and $F > F_{crit}$, so it can conclude that the concentration of SO_2 gas treatment affects the signal output generated by the sensor.

Tukey's yardstick method was used to determine whether there is a significant difference between the sensor's output signal at each SO_2 concentration treatment. To create the comparison matrix displayed in Table 8, this method compares the average response signal at each concentration level (AMS). The equation for Tukey's yardstick value will be return ω of 77.41. This value is added to the sensor's AMS so that the range value (AMS + ω) is formed (Table 7). At a concentration of 5 ppm, the range value is 77.41+32.40=109.81. If the AMS value at a concentration of 10 ppm is greater than the range value, the sensor output value at a concentration of 5 ppm-10 ppm is significantly

Table 5: Peak-stable value sensor response in millivolt.

Sensor	Repetition	The concentration of SO_2 gas (ppm)							
		5	10	20	30	40	50	60	70
Sensor-1	1	43.06	140.23	221.54	324.79	426.95	542.21	572.77	562.10
	2	26.65	134.12	200.01	283.03	348.33	519.89	527.80	537.60
	3	20.99	137.20	182.28	264.33	354.21	491.29	559.46	497.16
Sensor-2	1	31.94	97.64	221.00	308.64	400.22	506.80	510.44	540.28
	2	27.85	117.29	208.00	294.77	360.84	503.81	452.82	500.02
	3	33.19	112.39	203.51	276.71	351.68	482.65	479.16	507.25
Sensor-3	1	46.62	117.19	230.77	301.21	449.25	507.04	557.14	537.79
	2	32.67	122.18	192.83	285.64	409.72	504.21	496.89	507.73
	3	28.96	136.83	174.52	267.02	395.63	472.82	514.43	471.84

Table 6: Results of the ANOVA for each sensor for each iteration at each concentration level of SO_2 ($\alpha = 0.05$).

Source of Variation	SS	df	MS	F	P-value	F crit
Sample	3201.86	2	1600.93	3.02	0.0584	3.1907
Columns	2274017.98	7	324859.71	612.03	1.15E-44	2.2074
Interaction	12376.00	14	884.00	1.67	0.096	1.9037
Within	25477.95	48	530. 79			
Total	2315073.79	71				

different. This process is continued for a concentration of 10-20 ppm, 20-30 ppm, and so on.

Analysis of Linear Regression

In Table 8, the value "1", shows the significant difference between the average sensor output signal at a certain concentration level and the average value of the output signal at a certain concentration level. Meanwhile, the value "0" indicates the opposite meaning. For example, the ratio of the average response of a sensor signal at a concentration level of 50-60 ppm, 60-70 ppm, and 50-70 ppm are "0". This means that the signal in the concentration treatment is not significantly different. Thus it can be concluded that the sensor can only read SO_2 gas concentrations below 50 ppm.

CONCLUSION

Table 7: The mean and standard deviation of ANOVA for each sensor for each replication at each level of SO_2 concentration.

SO_2 (ppm)	Sensor-1		Sensor-2		Sensor-3		Average of the mean (AMS*)
	Mean	SD	Mean	SD	Mean	SD	
5	30.2	11.5	30.1	2.8	36.1	9.3	32.4
10	137.1	3.1	109.1	10.2	125.4	10.2	123.9
20	191.2	19.6	210.7	9.2	199.4	28.7	200.4
30	290.7	31.0	293.4	16.0	284.6	17.1	289.6
40	376.5	43.8	370.9	25.8	418.2	27.8	388.5
50	517.8	25.5	497.8	13.2	494.7	19.0	503.4
60	553.3	23.1	480.8	28.9	522.8	31.0	519.0
70	532.3	32.8	515.9	21.5	505.8	33.0	518.0

*AMS (Average of mean response signal at each concentration level)

Table 8: Matrix compares the total value of the average response signal with the range values calculated by Tukey's yardstick.

SO_2 concentration (ppm)	5	10	20	30	40	50	60	70
5	0	1	1	1	1	1	1	1
10		0	1	1	1	1	1	1
20			0	1	1	1	1	1
30				0	1	1	1	1
40					0	1	1	1
50						0	0	0
60							0	0
70								0

The calibration findings reveal that the sensor output signal and the SO_2 concentration treatment have a link. The coefficients of determination for sensor-1, sensor-2, and sensor-3 are 0.94, 0.91, and 0.93, respectively (Fig. 15). The MQ-136

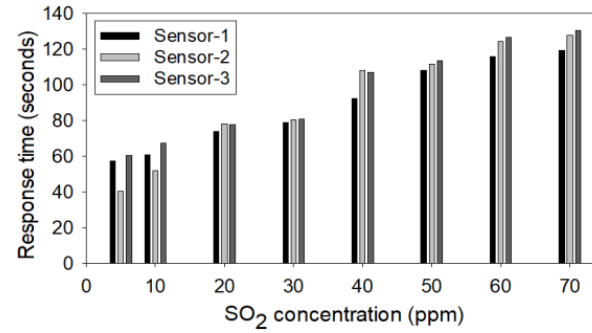

Fig.13: The average response time of the MQ-136 for each repetition of each level concentration SO_2 gas.

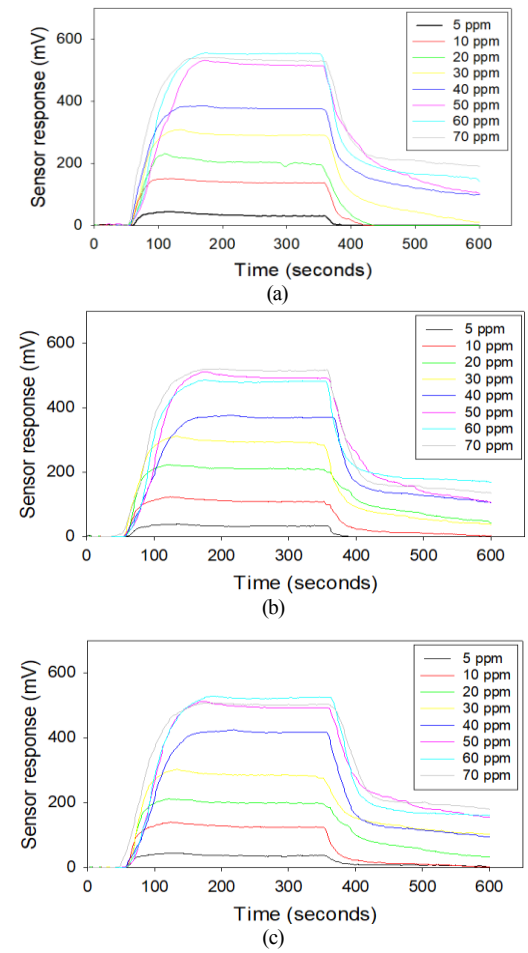

Fig. 14: Sensor response correction of each sensor MQ-136, sensor-1 (a), sensor-2 (b), and sensor-3 (c).

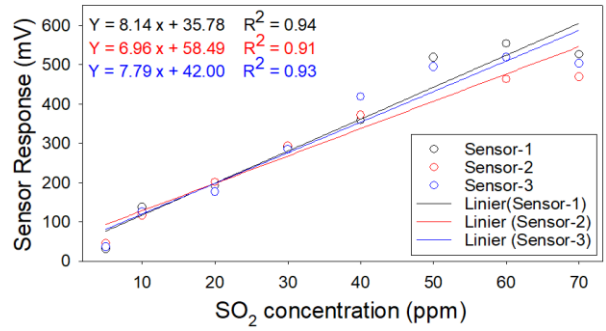

Fig. 15: The coefficient of determination of the effect of SO_2 gas concentration on the sensor response signal.

sensor utilized in this investigation, however, has an optimal reading range in the SO2 concentration range of 5 to 50 ppm, according to the ANOVA analysis results. Furthermore, the calibration findings reveal that the three MQ-136 sensors perform similarly. This is based on an ANOVA analysis that found no significant differences between the sensors.

ACKNOWLEDGMENTS

This research was supported by the Unilab Perdana Laboratory in a collaborative program with IPB University.

REFERENCES

Adithyan, R., Mohammed, A., Naseer, F.M., Ganesh, G., Nema, T., Sharma, P. and Mishra, V. 2016. Auto-Calibration of MOS gas sensor based on goodness of fit algorithm. Int. J. Adv. Sci. Eng. Technol., 4(2): 98-101.

Ahmed, S. 2015. Air pollution and its impact on agricultural crops in developing countries: A review. J. Anim. Plant Sci., 25(3): 297-302.

Arroyo, P., Herrero, J.L., Suárez, J.I. and Lozano, J. 2019. Wireless sensor network combined with cloud computing for air quality monitoring. Sensors (Switzerland), 19(3): 691. doi:10.3390/s19030691

Barsan, N., Weimar, U. and Chemistry T. 2012. Fundamentals of metal oxide gas sensors. Int. Meet. Chem. Sensors, 51: 618-621 .doi:10.5162/IMCS2012/7.3.3

Bassey, E., Whalley, J. and Sallis P. 2014. An evaluation of smoothing filters for gas sensor signal cleaning. Int. Conf. Adv. Commun. Comput., 21(1): 19-23.

Rawlings, J.O., Pantula, S.G. and Dickey, D.A. 1998. Applied Regression Analysis: A Research Tool. Springer, New York

Kim, S. and Kim, H. 2016. A new metric of absolute percentage error for intermittent demand forecasts. Int. J. Forecast, 32(3): 669-679.doi:10.1016/j.ijforecast.2015.12.003

Korotcenkov, G. 2007. Metal oxides for solid-state gas sensors: What determines our choice? Mater. Sci. Eng. B Solid-State Mater. Adv. Technol., 139(1): 1-23. doi: 10.1016/j.mseb.2007.01.044

Liu, X., Cheng, S., Liu, H., Hu, S., Zhang, D. and Ning, H. 2012. A survey on gas sensing technology. Sensors (Switzerland), 12(7): 9635-9665. doi:10.3390/s120709635

Riordan, D. and Adeeb, F. 2004. Air quality monitoring for sulfur dioxide in metropolitan Adelaide. Environ. Prot. Auth., 7: 27 https://www.epa.sa.gov.au/files/477254_so2_repo

Rumana, H.S., Sharma, R.C., Beniwal, V. and Sharma, A.K. 2014. A retrospective approach to assess human health risks associated with growing air pollution in the urbanized area of Thar Desert, Western Rajasthan, India. J. Environ. Health Sci. Eng., 12: 23. doi.org/10.1186/2052-336X-12-23

Samad, A., Nuñez, D.R.O., Castillo, G.C.S., Laquai, B. and Vogt, U. 2020. Effect of relative humidity and air temperature on the results obtained from low-cost gas sensors for ambient air quality measurements. Sensors (Switzerland), 20(18): 1-29. doi:10.3390/s20185175

Snyder, E.G., Watkins, T.H., Solomon, P.A., Thoma, E.D., Williams, R.W., Hagler, G.S.W., Shelow, D., Hindin, D.A., Kilaru, V.J. and Preuss, P.W. 2013. The changing paradigm of air pollution monitoring. Environ. Sci. Technol., 47(20):11369-11377.doi:10.1021/es4022602

Tian, F., Yang, S.X. and Dong, K. 2005. Circuit and noise analysis of odorant gas sensors in an E-nose. Sensors, 5(1-2): 85-96. doi:10.3390/s5010085

Zhengzhou, W.E.T. 2015. Manual for Hydrogen Sulfide Gas Sensor Model MQ136 version 1.4. Springer, NewYork